



**DEFORMATIONAL ANALYSIS
FOR REINFORCED CONCRETE BLOCKWORK BEAMS**

Songbo Li¹, A.N. Fried² and J.J. Roberts³

ABSTRACT

The results of a series of tests on reinforced concrete blockwork (RCB) beams carried out at the British Cement Association have been analyzed. Based on these test results and statistical analysis, the relationship between the stiffness of the beams and their deformation is examined enabling the deformation of RCB beams to be predicted.

INTRODUCTION

Although much research work has been carried out on the strength properties of masonry, few workers have considered how masonry deforms. The high variations that result from tests which examine the deflection of structural masonry have contributed to the difficulties in interpreting results.

A series of tests on reinforced concrete blockwork beams were carried out at the British Cement Association using a two point loading system (Roberts, 1992). Single course, two course and soldier course beams were included to investigate a number of properties of RCB beams including their deformation.

In any analysis of the deformation of a material, the stiffness (defined in this paper as EI) and how it changes, and the position of the neutral axis are critical. Since masonry is brittle and because the composite exhibits large variations in test results the determination of an accurate E value, stiffness, how these properties change with load, and

¹ Researcher, School of Civil Engineering, Kingston University, Surrey KT1 2EE, UK

² Senior Lecturer, School of Civil Engineering, Kingston University, Surrey KT1 2EE, UK

³ Professor and Dean of Faculty of Technology, Kingston University, Surrey KT1 2EE, UK

the position of the neutral axis will be complicated.

Analysis of the test results has enabled the relationship between the stiffness and deformation of the beams to be determined. Using this data the position of the neutral axis of the beams and the location of the point at which behaviour changes from elastic to elasto-plastic can be determined.

Table 1 Beam Properties

Beam no.	Beam ³ type	Mean comp. stgth. of infill N/mm ²	Mortar stgth. N/mm ²	Rein.	Eff. depth (mm)	Shear span / eff. depth a_v/d	Span (mm)
77 ¹	Two course	21.3	11.8	2T20	320	1.5	1860
80 ¹		18.9	12.5	"	"	3.0	2820
83 ¹	"	17.5	17.4	2T12	"	1.5	1860
86 ¹	"	15.7	13.3	"	"	3.0	2820
89 ¹	"	15.3	21.9	2T25	"	1.5	1860
92 ¹	"	16.3	18.0	"	"	3.0	2820
96 ¹	"	18.2	17.8	2T12	"	5.0	4100
97 ¹	"	19.1	19.9	2T20	"	5.0	4100
98 ¹	"	16.1	19.0	2T25	"	5.0	4100
99 ¹	"	14.8	19.3	2T16	"	5.0	4100
100 ¹	"	17.1	20.5	3T25	"	5.0	4100
101 ²	"	57.1	21.1	2T20	"	1.5	1860
102 ²	"	55.9	23.5	"	"	2.5	2500
103 ^{2*}	"	57.1	21.1	"	"	3.5	3140
104 ^{2*}	"	53.3	18.4	"	"	4.5	3750
105 ²	Sold-ier course	57.3	21.0	"	"	1.5	1860
106 ^{2*}		56.5	25.3	"	"	2.5	2500
107 ^{2*}	"	53.5	17.1	"	"	3.5	3140
108 ^{2*}	"	49.4	15.4	"	"	4.5	3750
109 ^{2*}	Single course	54.8	19.7	2T12	125	1.7	1320
110 ^{2*}		53.3	23.0	"	"	2.5	1525
111 ^{2*}	"	53.5	16.2	"	"	3.5	1775
112 ^{2*}	"	46.4	17.7	"	"	4.5	2025
113 ^{2*}	"	54.8	17.8	"	"	5.5	2275

Notes 1 - Block type 1, 15.4 N/mm².

2 - Block type 2, 44.6 N/mm².

3 - See Fig.1.

* - Stiffness/deflection relationship as in Fig.2b.

MATERIALS PROPERTIES

A U shaped dense aggregate concrete block was used in all the

beams. The blocks were 190x190x390 mm in size, obtained from a single supplier and as indicated in Table 1 two different strengths were used.

The mean net compressive strength of ten blocks of each strength grade was obtained by testing to BS 6073 (BSI, 1981). The mean net compressive strength for block type 1 was 15.4 N/mm² with a standard deviation of 0.9 N/mm² and coefficient of variation of 5.8%; for block type 2 the mean net compressive strength was 44.6 N/mm² with a standard deviation of 2.6 N/mm² and a coefficient of variation of 5.8%.

Mortar designation [i] was used throughout the programme in accordance with BS 5628 (BSI, 1985) and consisted of ordinary Portland cement, lime and building sand in the proportions 1 : 1/4 : 3 by volume. Three 100 mm cubes were made from each batch of mortar, subsequently cured and tested at 28 days in accordance with BS 1881 (BSI, 1983). The mean compressive strength of the mortar for each beam is indicated in Table 1. The overall mean compressive strength of mortar used with type 1 blocks was 17.8 N/mm² with a standard deviation of 3.6 N/mm² and coefficient of variation 20%. The mortar used with type 2 blocks had an overall mean compressive strength of 19.8 N/mm² with a standard deviation of 3.0 N/mm² and coefficient of variation of 15%.

Two different concrete mixes were used to fill the cores of the beams, each of which was designed to have a mean strength equal to the mean net strength of the block. Three 100 mm cubes were made from each batch of concrete and subsequently cured and tested at 28 days in accordance with BS 1881 (BSI, 1983). For the lower strength infill used with beam 76 - 100, the mean compressive strength was found to be 16.8 N/mm² with a standard deviation of 2.0 N/mm² and coefficient of variation of 12%. The corresponding figures for the higher strength infill (beam 101 - 113) were 54.1 N/mm², 3.2 N/mm² and 5.9% respectively. The mean compressive strengths of the infill concrete are given in Table 1.

High yield steel bars were placed in the U shaped cores to give the effective depth shown in Table 1 which also indicates their number, type and diameter. Specimens of reinforcement were tested in tension to obtain the ultimate strength.

Beams were constructed as single, double or soldier course. Details of all beams are given in Table 1 whilst typical beams and the two point loading system with a fixed length of constant moment is shown in Fig.1. The shear span was varied to give a number of different ratios of shear span/effective depth, thus resulting in beams of various lengths.

TESTING PROCEDURE

All beams were tested 28 days after placing the concrete infill. The test cycle was as follow:

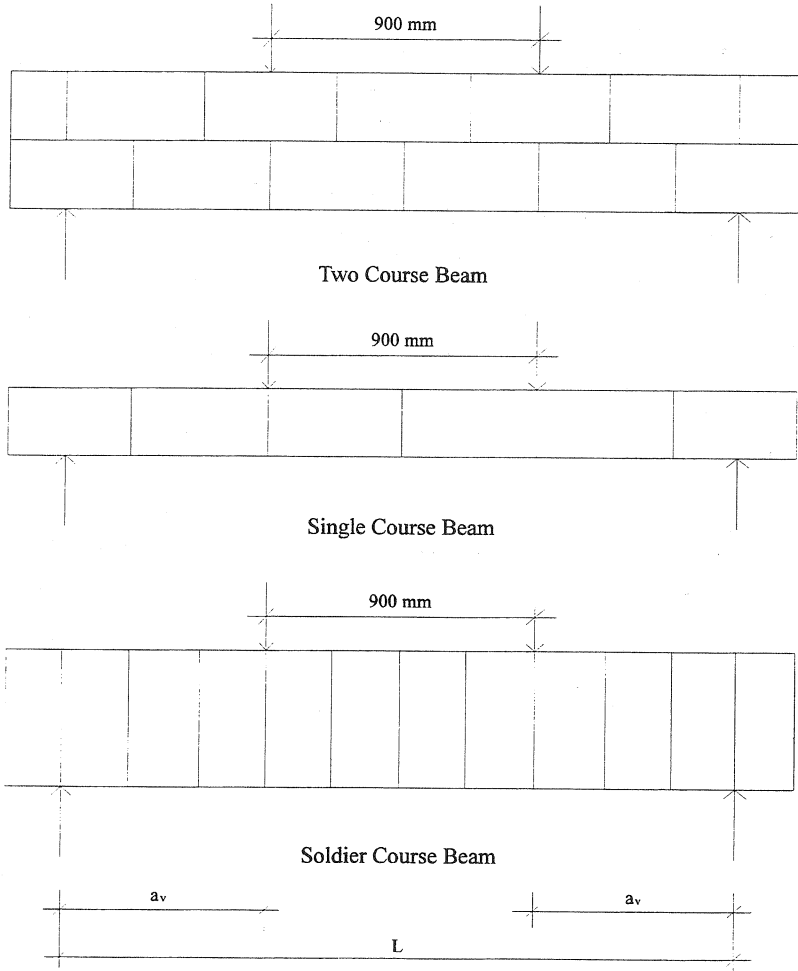


Fig.1 Test Configuration

The beams were lifted onto bearings in the test rig which gave simple support conditions. The span varied depending on the

shear span/effective depth ratio of the beam (see Fig.1).

Load was applied 450 mm either side of the beam centre line and, for the two course beams, care was taken to ensure the same configuration of blocks in the constant moment region in all cases.

The load was applied using two jacks acting directly on load cells coupled with a system of saddles and MacAlloy bars. Thus, the total applied moments and shear forces were provided by a uniformly distributed load due to the self weight of the specimens plus two point loads due to the applied load and the self weight of the loading apparatus.

The applied load was raised incrementally until failure occurred in flexure or shear. When failure occurred in one of the shear spans, no attempt was made to bring about a second failure in the other shear span.

STIFFNESS AND PREDICTION OF DEFORMATION

Results from the tested beams were used in equation [1] (Writing Group, 1975) to obtain the stiffness of the beams at each increment of load. Equation [1] is equivalent to that suggested in the Handbook to BS 5628 : Part 2 (Roberts et al 1986).

$$f = \frac{Pa_v L^2}{24EI} \left(3 - 4 \frac{a_v^2}{L^2}\right) + \frac{5qL^4}{384EI} \quad [1]$$

Where, f is the deformation;

P is the load applied on the beam as shown in Fig.1;

L is the support span as shown in Fig.1;

a_v is the distance between support and loading point;

q is the uniformly distributed load due to self weight;

E is the modulus of elasticity;

I is the moment of inertia.

Comparisons and Analyses of Stiffness

Table 2 shows the stiffness of each beam calculated using equation [1] at the first crack and ultimate loads and their a_v/d ratio. Each group of specimens in this Table uses similar blocks, is constructed in the same configuration with equal quantities of reinforcement. From Table 2, it is evident that, when a_v/d increases, the stiffness increases. The only exceptions are beams 112 and 113 in group 5. The decrease in stiffness in beam 112 is probably due to the lower strength of infill material. With beam 113, the high a_v/d coupled with the low percentage of reinforcement in the beam may have reduced the stiffness slightly.

Table 2

Beam no.	Group	a_v/d	EI, cracking point (N-mm ²)	EI, ultimate point (N-mm ²)
77	1	1.5	2.36×10^{13}	3.64×10^{12}
80	1	3.0	1.42×10^{14}	3.88×10^{13}
97	1	5.0	6.07×10^{14}	1.06×10^{14}
83	2	1.5	8.26×10^{13}	6.97×10^{12}
86	2	3.0	1.27×10^{14}	3.21×10^{13}
96	2	5.0	1.93×10^{15}	1.27×10^{14}
101	3	1.5	6.63×10^{13}	7.03×10^{12}
102	3	2.5	1.87×10^{14}	2.07×10^{13}
103	3	3.5	3.47×10^{15}	4.86×10^{13}
104	3	4.5	8.06×10^{15}	7.95×10^{13}
105	4	1.5	1.16×10^{14}	9.36×10^{12}
106	4	2.5	2.45×10^{15}	3.47×10^{13}
107	4	3.5	6.37×10^{15}	5.51×10^{13}
108	4	4.5	1.32×10^{16}	9.91×10^{13}
109	5	1.7	3.42×10^{13}	8.55×10^{11}
110	5	2.5	4.05×10^{13}	1.32×10^{12}
111	5	3.5	1.73×10^{14}	3.26×10^{12}
112	5	4.5	1.05×10^{14}	2.05×10^{12}
113	5	5.5	1.79×10^{14}	3.03×10^{12}

Table 3 shows the stiffness of each beam at the first crack and ultimate loads and their material strength. The material strength is a function of the strength of blocks, mortar, concrete infill and the percentage of infill in the beam. Each group of specimens in Table 3 is constructed in the same configuration, has the same quantity of reinforcement and equal a_v/d ratios. The Table indicates that, when material strength increases, the stiffness at the cracking load increases too, but the stiffness at ultimate load is unchanged. Up to the cracking load, the masonry and reinforcement act together elastically, whereas after cracking the masonry resists the compressive loads whilst the reinforcement carries tensile loads. The ductility of the steel which governs behaviour at ultimate load probably accounts for the stiffness being unchanged.

Table 4 shows the effect of reinforcement on stiffness. Each group of specimens in this Table is constructed in the same configuration, has the same material strength, and equal a_v/d ratios. As expected, the stiffness at cracking loads are independent of the quantity of reinforcement whereas at ultimate load, there is some indication that the stiffness increases with area of reinforcement although this factor will

also be influenced by the span and a_v/d ratio.

Table 3

Beam no.	Group	Material strength (N/mm ²)	EI, cracking point (N-mm ²)	EI, ultimate point (N-mm ²)
77	1	12.367	2.36×10^{13}	3.64×10^{12}
101	1	35.063	6.63×10^{13}	7.03×10^{12}
80	2	12.256	1.42×10^{14}	3.88×10^{13}
102	2	34.614	1.87×10^{14}	2.07×10^{13}
80	3	12.256	1.42×10^{14}	3.88×10^{13}
103	3	35.063	3.47×10^{15}	4.86×10^{13}
97	4	12.771	6.07×10^{14}	1.06×10^{14}
104	4	32.883	8.06×10^{15}	7.95×10^{13}

Table 4

Beam no.	Group	Reinforcement	EI, cracking point (N-mm ²)	EI, ultimate point (N-mm ²)
83	1	2T12	8.26×10^{13}	6.97×10^{12}
77	1	2T20	2.36×10^{13}	3.64×10^{12}
89	1	2T25	3.11×10^{13}	1.02×10^{13}
86	2	2T12	1.27×10^{14}	3.21×10^{13}
80	2	2T20	1.42×10^{14}	3.88×10^{13}
92	2	2T25	1.54×10^{14}	4.35×10^{13}
96	3	2T12	1.93×10^{15}	1.27×10^{14}
99	3	2T16	1.07×10^{15}	1.36×10^{14}
97	3	2T20	6.07×10^{14}	1.06×10^{14}
98	3	2T25	7.67×10^{14}	1.33×10^{14}
100	3	3T25	9.71×10^{14}	1.60×10^{14}

Table 5 shows the effect of beam configuration on stiffness. Each group of specimens has similar material strength, the same amount of reinforcement and equal a_v/d ratios. The Table indicates the stiffness of two course beams are always less than those of soldier course beams. However the stiffness of soldier course beams drops more rapidly than the two course specimens as loads increase above cracking. Greater post cracking stiffness occurs in the two course beams because vertical debonding at the first cracking load occurs through the perpend in the two course beams and is halted at the beam mid height when the joint intercepts the centre of a unit in the top row whereas in the soldier course beams cracking will be in a vertical joint and hence unrestricted.

Table 5

Beam no.	Group	Beam type	EI, cracking point (N-mm ²)	EI, ultimate point (N-mm ²)
101	1	Two course	6.63×10^{13}	7.03×10^{12}
105	1	Soldier	1.16×10^{14}	9.36×10^{12}
102	2	Two course	1.87×10^{14}	2.07×10^{13}
106	2	Soldier	2.45×10^{15}	3.47×10^{13}
103	3	Two course	3.47×10^{15}	4.86×10^{13}
107	3	Soldier	6.37×10^{15}	5.51×10^{13}
104	4	Two course	8.06×10^{15}	7.95×10^{13}
108	4	Soldier	1.32×10^{16}	9.91×10^{13}

Stiffness / Deformation Relationships

Fig.2 shows the relationship between the stiffness and deflection of the beams. Two groups of specimens each exhibiting different characteristics are shown. In group A (Fig.2a), initially no loss of stiffness occurred after which an exponential type of decay was noted. In group B (Fig.2b), a very rapid decay to about one tenth of the maximum initial value occurred from very low loads after which the drop was gentle. The beams marked with an "*" in Table 1 represent group B and include almost all of the soldier and single course beams, whereas group A included almost all the two course beams. The exceptions are beams 103, 104 and 105.

Group A predominantly comprises two course beams. Initial cracking in the flexural zone extends upwards from the beam soffit but is halted at the beam mid height when the perpend is intercepted by a unit in the top course. This ensures the zone in compression after initial cracking will not reduce in size as further cracking is prevented. Consequently the rate at which the neutral axis will progress upwards as the loading increases will be dependent on the elastic properties of the top course, in relationship to the reinforcement. With the single and soldier course beams no such restriction to the initial crack exists and the movement of the neutral axis will be as for a cracked member.

As mentioned, beams 103, 104 and 105 are the exceptions. Beams 103 and 104 are two course beams with higher material strength. However, it appears that the higher span/depth ratios of these beams is more important in forcing these elements into group B than the material strength. Flexural cracks through the perpend induced sufficient strains in the upper course to cause the initial crack to extend into the top course of the beams. With beam 105, the low span/depth ratio and relatively high quantity of reinforcement have resulted in

the section behaving as an over reinforced beam.

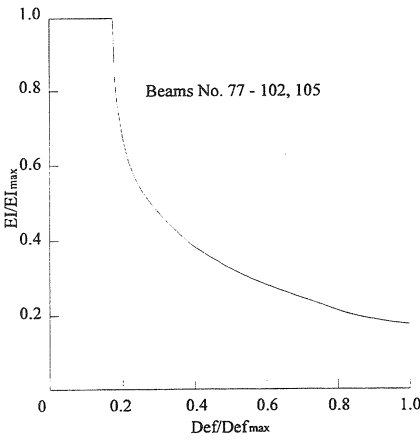


Fig.2a (group A)

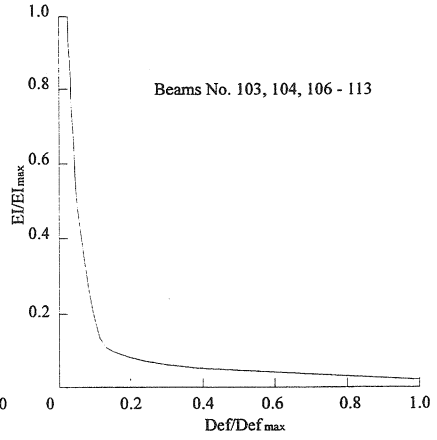


Fig.2b (group B)

Fig.2

Prediction of Deformation for RCB Beams

The measured central deformations of the RCB beams are shown in Table 6 together with deflections based on elasticities derived from the Chinese, British and European codes of practice. There are also estimates of deflections based on the stress block derived by Roberts (Roberts, 1975). The equations are shown below.

$$d_n = 0.108l^2 \left(\frac{M_c}{\sum EI} \right) + 0.104l^2 \left(\frac{M_{DL}}{\sum EI} \right) \quad [2]$$

Where l is the distance between supports;
 M_c is the maximum moment due to live load;
 M_{DL} is the maximum moment due to dead load;
 and

$$\sum EI = \frac{bd_c^3 E_b}{4} + A_s (d_1 - d_c)^2 E_s$$

where b is the width of the beam;
 d_c is the depth to neutral axis;
 d_1 is the depth to tensile reinforcing steel;
 A_s is the area of tensile reinforcing steel;
 E_b is the modulus of elasticity of blockwork system;
 E_s is the modulus of elasticity of reinforcing steel.

Here

$$\frac{bd_c^2}{2} = mA_s(d-d_c) \quad [3]$$

where m is the modular ratio of steel to blockwork system;
 d is the depth to reinforcement.

In the other cases, the stiffness of the beam and the depth of the neutral axis were determined by equations [1], [4] and [5] in accordance with elastic theory.

$$EI = \frac{bd_c^3}{3} E_m + A_s(d-d_c)^2 E_s \quad [4]$$

and

$$d_c = K \frac{f_y}{f_k} Qd \quad [5]$$

In which,

$$Q = \frac{A_s}{bd}$$

Here, E_m is the modulus of elasticity of masonry;
 E_s is the modulus of elasticity of reinforcement;
 d_c is the depth to neutral axis;
 A_s is the section area of reinforcement;
 f_y is the strength of reinforcement;
 f_k is the strength of masonry;
 b is the width of beam;
 d is the effective depth of beam;
 K is a coefficient dependent on the values of f_y and f_k .
As f_y and f_k vary from code to code, so the value of K will differ as follows. In BS 5628, $K=1/0.35$; in GBJ 3-73, $K=1/0.4$; in EC 6, $K=1/0.6$. Using the calculated K , a value of d_c and EI was then found for every beam using elastic theory, from which the central deformation of each beam was recalculated. These values are in Table 6.

The Table indicates that the most reliable prediction of deflection is to use the technique suggested by Roberts.

CONCLUSIONS

The stiffness of RCB beams increases as the a_v/d ratio increases.

Increased material strengths resulted in higher beam stiffness at cracking load but had little impact on the stiffness at

ultimate load.

Table 6 Deflections at Beam Centre (mm)

Beam no.	Test	Roberts	GBJ 3-73	BS 5628	EC 6
77	9.6	2.2	1.8	1.6	1.9
80	12.7	9.2	25.6	22.1	26.3
83	10.1	5.1	22.8	23.6	27.8
86	14.8	11.8	155.0	160.2	188.7
89	8.9	4.8	1.2	1.0	1.1
92	11.5	8.2	6.6	5.5	6.1
96	23.1	23.4	-	-	-
97	28.3	25.0	156.3	135.0	160.7
98	22.7	20.9	40.0	33.2	36.8
99	21.9	24.4	451.9	428.1	539.4
100	18.9	17.5	10.8	8.9	9.5
101	12.6	3.9	9.7	10.4	12.5
102	14.4	6.8	32.5	35.0	41.9
103	17.4	11.1	92.1	99.3	118.9
104	24.8	16.7	214.6	231.4	277.3
105	9.9	4.4	10.1	10.9	13.1
106	8.5	6.4	32.1	34.6	41.5
107	15.7	13.6	94.2	101.6	121.7
108	20.0	18.1	215.7	232.6	278.7
109	9.8	6.8	16.3	17.6	21.0
110	10.9	8.5	27.9	30.2	35.9
111	14.0	17.7	88.9	95.9	114.3
112	24.0	14.8	95.8	103.5	123.2
113	27.8	18.5	163.9	176.9	210.7

The stiffness of RCB beams before cracking are independent of the quantity of reinforcement whereas at ultimate load there is an increase in stiffness as the quantity of reinforcement increases.

The stiffness of two course beams is less than that of soldier course beams.

The drop in stiffness after cracking is more rapid in soldier than two course beams.

Two course beams maintain their initial stiffness to higher loads than soldier course beams.

The deformation of RCB beams can be predicted with reasonable reliability using the technique suggested by Roberts. The predictions are less reliable in beams with low a_v/d ratios.

REFERENCES

- British Standard Institution (1981), BS 6073: Precast Concrete Masonry Unit: Part 1: 1981, latest amendment February 1984, BSI, London, UK.
- British Standard Institution (1983), BS 1881: Testing Concrete: Part 116: 1983, latest amendment July 1991, BSI, London, UK.
- British Standard Institution (1985), BS 5628: Code of Practice for Use of Masonry: Part 2: 1985, BSI, London, UK.
- British Standard Institution (1985), BS 5628: Code of Practice for Use of Masonry: Part 3: 1985, latest amendment November 1985, BSI, London, UK.
- British Standard Institution (1985), BS 8110: Structural Use of Concrete: Part 1: 1985, latest amendment September 1993, BSI, London, UK.
- British Standard Institution (1992), BS 5628: Code of Practice for Use of Masonry: Part 1: 1992, latest amendment July 1993, BSI, London, UK.
- Commission of the European Communities (1988), Eurocode No.6: Common Unified Rules for Masonry Structures, ECC, Batiment Jean Monnet, Luxembourg.
- Construction Ministry of China (1973), National Standard of P.R. China, GBJ 3-73: Design Code of Masonry Structures, CM, Beijing, China.
- Roberts, J.J. (1975), The Behaviour of Vertically Reinforced Concrete Blockwork Subject to Lateral Loading, Technical Report, ISBN 0 7210 1004 0, Cement and Conc. Ass., London, UK.
- Roberts, J.J., Tovey, A.K., Cranston, W.B. and Beeby, A.W. (1983), Concrete Masonry Designer's Handbook, Eyre & Spottiswoode Publications Ltd, Leatherhead, UK.
- Roberts, J.J., Edgell, G.J. and Rathbone, A.J. (1986), Handbook to BS 5628 : Part 2, Palladian Publications Limited, London, UK.
- Roberts, J.J. (1992), The Shear Behaviour of Reinforced Concrete Blockwork Beams, Proceedings of the 3rd International Masonry Conference, British Masonry Society, London, UK.
- Writing Group (1975), Static Calculation Handbook of Building Structures, the Publishing House of Construction Industry of China, Beijing, China.